

CHAPTER II

**RADIATION AND MASS TRANSFER EFFECTS ON MHD FREE
CONVECTIVE FLOW OF A MICROPOLAR FLUID PAST AN INFINITE
VERTICAL POROUS MOVING PLATE EMBEDDED IN A POROUS MEDIUM
WITH VISCOUS DISSIPATION**

1. INTRODUCTION

Simultaneous heat and mass transfer from different geometries embedded in porous media has many engineering and geophysical applications such as geothermal reservoirs, drying of porous solids, thermal insulation, enhanced oil recovery, packed-bed catalytic reactors, cooling of nuclear reactors, and under ground energy transport. Cheng and Minkowycz [1] presented similarity solutions for free thermal convection from a plate in a fluid-saturated porous medium. Bejan and Khair [2] reported on the natural convection boundary layer flow in a saturated porous medium with combined heat and mass transfer. Lai and Kulacki [3] extended the problem of Bejan and Khair [2] to include wall fluid injection effects. Bestman [4] examined the natural convection boundary layer with suction and mass transfer in a porous medium. In all these studies the fluids are assumed to be Newtonian.

In recent years, the dynamics of micropolar fluids has been a popular area of research. As the fluids consist of randomly oriented molecules, and as each volume element of the fluid has translation as well as rotation motions, the analysis of physical problems in these fluids has revealed several interesting phenomena, which are not found in Newtonian fluids. The theory of micropolar fluids and thermo micropolar fluids developed by Eringen [5, 6] can be used to explain the characteristics in certain fluids such as exotic lubricants, colloidal suspensions, or polymeric fluids, liquid crystals and animal blood. The micropolar fluids exhibit certain microscopic effects arising from local structure and microrotation of fluid elements. An excellent review about micropolar fluid mechanics was provided by Ariman et al. [7, 8].

The study of flow and heat transfer of an electrically conducting micropolar fluid past a porous plate under the influence of a magnetic field has attracted the interest of numerous researchers in view of its applications in many engineering problems, such as MHD generators, nuclear reactors, geothermal energy extractions and the boundary layer control in the field of aerodynamics. Keeping in mind some specific industrial applications such as polymer processing technology, numerous attempts have been made to analyze the effect of transverse magnetic field on boundary layer flow characteristics. Mansour and Gorla [9] reported on micropolar fluid flow past a continuously moving in the presence of magnetic field. El-Hakim et al. [10] have studied Joule heating effects

on MHD free convection flow of a micropolar fluid. El-Amin [11] solved the problem of MHD free convection and mass transfer flow in a micropolar fluid with constant suction. Helmy et al. [12] have studied on MHD free convection flow of a micropolar fluid past a vertical porous plate. Seddeek [13] reported the flow of a micropolar fluid by the presence of magnetic field over a continuously moving plate. Kim [14] presented an unsteady MHD mixed convection with mass transfer flow for a micropolar fluid past a vertical moving porous plate via a porous medium.

For some industrial applications such as glass production and furnace design, and in space technology applications such as cosmical flight aerodynamics rocket, propulsion systems, plasma physics and spacecraft re-entry aerothermodynamics which operate at higher temperatures, radiation effects can be significant. Perdakis and Raptis [15] studied heat transfer of a micropolar fluid in the presence of radiation. Kim and Fedorov [17] analyzed transient mixed radiative convective flow of a micropolar fluid past a moving semi-infinite vertical porous plate. Later Raptis [16] studied the same fluid flow past a continuously moving plate in the presence of radiation. Recently, Rahman and Sattar [18] studied transient convective heat transfer flow of a micropolar fluid past a continuously moving vertical porous plate with time dependent suction in the presence of radiation. Cooney et al. [19] studied the influence of viscous dissipation and radiation on unsteady MHD free convection flow past an infinite heated vertical plate in a porous medium with time-dependent suction. Ramachandra Prasad and Bhaskar Reddy [20] investigated radiation and mass transfer effects on an unsteady MHD free convection flow past a heated vertical plate in a porous medium with viscous dissipation. Sankar Reddy et al. [21] reported unsteady MHD convective heat and mass transfer flow of micropolar fluid past a semi-infinite vertical moving porous plate in the presence radiation. Sankar Reddy et al. [22] have studied the problem of radiation effects on MHD mixed convection flow of a micropolar fluid past a semi-infinite moving porous plate in a porous medium with heat absorption.

Viscous dissipation, which appears as a source term in the fluid flow generates appreciable temperature, gives the rate at which mechanical energy is converted into heat in a viscous fluid per unit volume. This effect is of particular significance in natural convection in various devices that are subjected to large variation of gravitational force or

that operate at high rotational speeds, as pointed by Gebhart [23] in his study of viscous dissipation on natural convection in fluids. Similarity solution for the same problem with exponential variation of wall temperature was obtained by Gebhart and Mollendorf [24].

However, the effect of radiation and viscous dissipation on heat and mass transfer flow of a micropolar fluid has not received any attention. Hence, the objective of the present chapter is to study the effect of thermal radiation on magnetohydrodynamic free convection heat and mass transfer flow of a micropolar fluid past an infinite vertical porous moving plate embedded in a porous medium in the presence of viscous dissipation. The dimensionless governing equations of the flow, heat and mass transfer are solved analytically using a regular perturbation technique. Numerical results are reported in figures and tables, for various values of the physical parameters of interest.

2. MATHEMATICAL ANALYSIS

An unsteady two-dimensional laminar free convective flow of a viscous, incompressible, electrically conducting and micropolar fluid past an infinite vertical permeable moving plate, embedded in a uniform porous medium in the presence of thermal radiation and viscous dissipation is considered. The x' -axis is taken along the vertical plate and the y' -axis normal to the plate. A uniform magnetic field is applied in the direction perpendicular to the plate. The transverse applied magnetic field and magnetic Reynolds number are assumed to be very small and hence the induced magnetic field is negligible [25]. Also, it is assumed that there is no applied voltage, so that the electric field is absent. Since the plate is of infinite length, all the flow variables are functions of normal distance y' and time t' only. Now, under the usual Boussinesq's approximation, the governing boundary layer equations of the problem are

Continuity

$$\frac{\partial v'}{\partial y'} = 0 \quad (2.1)$$

Linear Momentum

$$\frac{\partial u'}{\partial t'} + v' \frac{\partial u'}{\partial y'} = (v + \nu_r) \frac{\partial^2 u'}{\partial y'^2} + g\beta_r(T' - T_w') + g\beta_c(C' - C_w') - \left(\frac{\sigma}{\rho} B_0^2 + \frac{\nu}{K'} \right) u' + 2\nu_r \frac{\partial \omega'}{\partial y'} \quad (2.2)$$

Angular Momentum

$$\rho j' \left(\frac{\partial \omega'}{\partial t'} + v' \cdot \frac{\partial \omega'}{\partial y'} \right) = \gamma \frac{\partial^2 \omega'}{\partial y'^2} \quad (2.3)$$

Energy

$$\frac{\partial T'}{\partial t'} + v' \frac{\partial T'}{\partial y'} = \alpha \left[\frac{\partial^2 T'}{\partial y'^2} - \frac{1}{k} \frac{\partial q'}{\partial y'} \right] + \frac{v'}{c_p} \left(\frac{\partial u'}{\partial y'} \right)^2 \quad (2.4)$$

Diffusion

$$\frac{\partial C'}{\partial t'} + v' \frac{\partial C'}{\partial y'} = D \frac{\partial^2 C'}{\partial y'^2} \quad (2.5)$$

where u', v' are the velocity components in x', y' directions respectively, t' - the time, ρ - the fluid density, g - the acceleration due to gravity, β_t and β_c the thermal and concentration expansion coefficients respectively, K' - the permeability of the porous medium, j' is the micro-inertia density, ω' is the component of the angular velocity vector normal to the $x'y'$ -plane, γ is the spin-gradient viscosity, T' - the temperature of the fluid in the boundary layer, ν - the kinematic viscosity, ν_r is the kinematic rotational velocity, σ - the electrical conductivity of the fluid, T_∞' - the temperature of the fluid far away from the plate, C' - the species concentration in the boundary layer, C_∞' - the species concentration in the fluid far away from the plate, B_0 - the magnetic induction, α - the fluid thermal diffusivity, k - the thermal conductivity, c_p is the specific heat at constant pressure, q' - the radiative heat flux and D - chemical molecular diffusivity. The second and third terms on the right hand side of the momentum equation (2.2) denote the thermal and concentration buoyancy effects respectively. Also, the last two terms on the right hand side of the energy equation (2.4) represents the radiative heat flux and viscous dissipation, respectively.

It is assumed that the permeable plate moves with a constant velocity in the direction of fluid flow. The appropriate boundary conditions for the velocity, microrotation, temperature and concentration fields are

$$u' = u'_p, \quad w' = -\frac{\partial u'}{\partial y'}, \quad T' = T_w, \quad C' = C_w \quad \text{at } y' = 0 \quad (2.6)$$

$$u' = U_\infty, \quad \omega' \rightarrow 0, \quad T' \rightarrow T_\infty, \quad C' \rightarrow C_\infty \quad \text{as } y' \rightarrow \infty$$

where u'_p is the plate velocity, T_w and C_w - the temperature and concentration of the plate respectively, U_∞ - the free stream velocity and U_0 and n' the constants.

By using Rosseland approximation (Brewster [26]), the radiative heat flux q_r is given by

$$q_r = \frac{-4\sigma_s \partial T'^4}{3K_s \partial y'} \quad (2.7)$$

where σ_s is the Stefan - Boltzmann constant and K_s - the mean absorption coefficient. It should be noted that by using the Rosseland approximation, the present analysis is limited to optically thick fluids. If temperature differences with in the flow are sufficiently small, then equation (2.6) can be linearised by expanding T'^4 into the Taylor series about T_w , which after neglecting higher order terms takes the form.

$$T'^4 \cong 4T_w^3 T' - 3T_w^4 \quad (2.8)$$

In view of equations (2.6) and (2.7), equation (2.4) reduces to

$$\frac{\partial T'}{\partial t'} + v' \frac{\partial T'}{\partial y'} = \frac{k}{\rho c_p} \frac{\partial^2 T'}{\partial y'^2} + \frac{16\sigma_s}{3\rho c_p K_s} \frac{\partial^2 T'}{\partial y'^2} + \frac{\mu}{\rho c_p} \left(\frac{\partial u'}{\partial y'} \right)^2 \quad (2.9)$$

It is clear from equation (2.1) that the suction velocity normal to the plate is a constant. Here, it is assumed to be

$$v' = -V_0 \quad (2.10)$$

where V_0 is the scale of suction velocity which is a non-zero positive constant. The negative sign indicates that the suction is towards the plate.

In order to write the governing equations and the boundary conditions in dimensionless form, the following non-dimensional quantities are introduced.

$$u = \frac{u'}{U_0}, \quad v = \frac{v'}{V_0}, \quad y = \frac{V_0 y'}{U_0}, \quad U_p = \frac{u_p}{U_0}, \quad n = \frac{n' V_0}{U_0}, \quad \omega = \frac{v}{U_0 V_0} \omega', \quad \beta = \frac{v}{v} \\ M = \frac{\sigma B_0^2 U_0}{\rho V_0^2}, \quad K = \frac{K' V_0^2}{v^2}, \quad I = \frac{I' V_0^2}{v}, \quad \theta = \frac{T - T_\infty}{T_w - T_\infty}, \quad C = \frac{C' - C_\infty}{C_w - C_\infty}$$

$$Gr = j = \frac{V_0^2}{\nu^2} j^*, \frac{\nu \beta_f g (T_w - T_\infty)}{U_0 V_0^2}, Gc = \frac{\nu \beta_c g (C_w - C_\infty)}{U_0 V_0^2}, \quad (2.11)$$

$$Pr = \frac{\nu \rho C_p}{k} = \frac{\nu}{\alpha} = \frac{\mu C_p}{k}, R = \frac{16 \sigma_1 T_w^3}{3 K_r k}, Ec = \frac{V_0^2}{C_p (T_w - T_\infty)}, Sc = \frac{\nu}{D}$$

Furthermore, the spin-gradient viscosity γ which gives some relationship between the coefficients of viscosity and micro-inertia, is defined as

$$\gamma = \left(\mu + \frac{\Lambda}{2} \right) j^* = \mu j^* \left(1 + \frac{1}{2} \beta \right); \beta = \frac{\Lambda}{\mu}; \quad (2.12)$$

In view of equations (2.10) - (2.12), equations (2.2), (2.3), (2.5) and (2.9) reduce to the following dimensionless form.

$$\frac{\partial u}{\partial t} - \frac{\partial u}{\partial y} = (1 + \beta) \frac{\partial^2 u}{\partial y^2} - Nu + G, \theta + G, C + 2\beta \frac{\partial \omega}{\partial y}, \quad (2.13)$$

$$\frac{\partial \omega}{\partial t} - \frac{\partial \omega}{\partial y} = \frac{1}{\eta} \frac{\partial^2 \omega}{\partial y^2}, \quad (2.14)$$

$$\frac{\partial \theta}{\partial t} - \frac{\partial \theta}{\partial y} = \frac{1}{\Gamma} \frac{\partial^2 \theta}{\partial y^2} + Ec \left(\frac{\partial u}{\partial y} \right)^2, \quad (2.15)$$

$$\frac{\partial C}{\partial t} - \frac{\partial C}{\partial y} = \frac{1}{Sc} \frac{\partial^2 C}{\partial y^2}. \quad (2.16)$$

where $\eta = \frac{\mu j^*}{\gamma} = \frac{2}{2 + \beta}, N = M + \frac{1}{K}, \Gamma = \left(1 - \frac{4}{3R + 4} \right) Pr$

and Gr, Gm, Pr, R, Ec and Sc are the thermal Grashof number, solutal Grashof Number, Prandtl Number, radiation parameter, Eckert number and Schmidt number, respectively.

The corresponding boundary conditions are

$$u = U_0, \omega = -\frac{\partial u}{\partial y}, \theta = 1, C = 1 \text{ at } y = 0 \quad (2.17)$$

$$u \rightarrow 0, \omega \rightarrow 0, \theta \rightarrow 0, C \rightarrow 0 \text{ as } y \rightarrow \infty$$

3. SOLUTION OF THE PROBLEM

In order to reduce the above system of partial differential equations to a system of ordinary differential equations, we perform an asymptotic analysis by representing the linear velocity, microrotation, temperature and concentration in the neighbourhood of the porous plate as

$$\begin{aligned}
u &= u_0(y) + \varepsilon e^{\alpha y} u_1(y) + O(\varepsilon^2) + \dots \\
\omega &= \omega_0(y) + \varepsilon e^{\alpha y} \omega_1(y) + O(\varepsilon^2) + \dots \\
\theta &= \theta_0(y) + \varepsilon e^{\alpha y} \theta_1(y) + O(\varepsilon^2) + \dots \\
C &= C_0(y) + \varepsilon e^{\alpha y} C_1(y) + O(\varepsilon^2) + \dots
\end{aligned} \tag{3.1}$$

Substituting equation (3.1) into equations (2.10)-(2.13), and equating the harmonic and non-harmonic terms, and neglecting the higher-order terms of $O(\varepsilon^2)$, we obtain the following pairs of equations for $(u_0, \omega_0, \theta_0, C_0)$ and $(u_1, \omega_1, \theta_1, C_1)$.

$$(1 + \beta)u_0'' + u_0' - Nu_0 = -G_0\theta_0 - G_0C_0 - 2\beta\omega_0' \tag{3.2}$$

$$(1 + \beta)u_1'' + u_1' - (N + n)u_1 = -G_0\theta_1 - G_0C_1 - 2\beta\omega_1' \tag{3.3}$$

$$\omega_0'' + \eta\omega_0' = 0 \tag{3.4}$$

$$\omega_1'' + \eta\omega_1' - n\eta\omega_1 = 0 \tag{3.5}$$

$$\theta_0'' + \Gamma\theta_0' = -\Gamma Ec(u_0')^2 \tag{3.6}$$

$$\theta_1'' + \Gamma\theta_1' - n\Gamma\theta_1 = -2\Gamma Ec u_0' u_1' \tag{3.7}$$

$$C_0'' + ScC_0' = 0, \tag{3.8}$$

$$C_1'' + ScC_1' - nScC_1 = 0 \tag{3.9}$$

where the primes denote differentiation with respect to y only.

The corresponding boundary conditions can be written as

$$\begin{aligned}
u_0 = U_p, u_1 = 0, \omega_0 = -u_0', \omega_1 = -u_1', \theta_0 = 1, \theta_1 = 0, C_0 = 1, C_1 = 0 \text{ at } y = 0 \\
u_0 = 0, u_1 = 0, \omega_0 \rightarrow 0, \omega_1 \rightarrow 0, \theta_0 \rightarrow 0, \theta_1 \rightarrow 0, C_0 \rightarrow 0, C_1 \rightarrow 0 \text{ as } y \rightarrow \infty
\end{aligned} \tag{3.10}$$

The equations (3.2) - (3.9) are still coupled and non-linear, whose exact solutions are not possible. So we expand $(u_0, \omega_0, \theta_0)$ and $(u_1, \omega_1, \theta_1)$ in terms of Ec in the following form, as the Eckert number is very small for incompressible flows.

$$\begin{aligned}
u_0(y) &= u_{01}(y) + Ec u_{02}(y), \quad u_1(y) = u_{11}(y) + Ec u_{12}(y), \\
\omega_0(y) &= \omega_{01}(y) + Ec \omega_{02}(y), \quad \omega_1(y) = \omega_{11}(y) + Ec \omega_{12}(y), \\
\theta_0(y) &= \theta_{01}(y) + Ec \theta_{02}(y), \quad \theta_1(y) = \theta_{11}(y) + Ec \theta_{12}(y).
\end{aligned} \tag{3.11}$$

Substituting (3.11) in equations (3.2) - (3.9), equating the coefficients of Ec to zero and neglecting the terms in Ec^2 and higher order, we get the following equations.

The zeroth order equations are

$$(1 + \beta)u_{01}'' + u_{01}' - Nu_{01} = -Gr\theta_{01} - GmC_{01} - 2\beta\omega_{01}' \quad (3.12)$$

$$(1 + \beta)u_{02}'' + u_{02}' - Nu_{02} = -Gr\theta_{02} - GmC_{02} - 2\beta\omega_{02}' \quad (3.13)$$

$$\omega_{01}'' + \eta\omega_{01}' = 0 \quad (3.14)$$

$$\omega_{02}'' + \eta\omega_{02}' = 0 \quad (3.15)$$

$$\theta_{01}'' + \Gamma\theta_{01}' = 0 \quad (3.16)$$

$$\theta_{02}'' + \Gamma\theta_{02}' = -\Gamma Ecu_{01}'^2 \quad (3.17)$$

and the corresponding boundary conditions are

$$u_{01} = U_p, u_{02} = 0, \theta_{01} = 1, \theta_{02} = 0, \omega_{01} = -u_{01}', \omega_{02} = -u_{02}' \text{ at } y = 0 \quad (3.18)$$

$$u_{01} \rightarrow 0, u_{02} \rightarrow 0, \theta_{01} \rightarrow 0, \theta_{02} \rightarrow 0, \omega_{01} \rightarrow 0, \omega_{02} \rightarrow 0 \text{ as } y \rightarrow \infty$$

The second order equations are

$$(1 + \beta)u_{11}'' + u_{11}' - Nu_{11} = -Gr\theta_{11} - GmC_{11} - 2\beta\omega_{11}' \quad (3.19)$$

$$(1 + \beta)u_{12}'' + u_{12}' - Nu_{12} = -Gr\theta_{12} - GmC_{12} - 2\beta\omega_{12}' \quad (3.20)$$

$$\omega_{11}'' + \eta\omega_{11}' - n\eta\omega_{11} = 0 \quad (3.21)$$

$$\omega_{12}'' + \eta\omega_{12}' - n\eta\omega_{12} = 0 \quad (3.22)$$

$$\theta_{11}'' + \Gamma\theta_{11}' - n\Gamma\theta_{11} = 0 \quad (3.23)$$

$$\theta_{12}'' + \Gamma\theta_{12}' - n\Gamma\theta_{12} = -2\Gamma Ecu_{01}'u_{11}' \quad (3.24)$$

and the corresponding boundary conditions are

$$u_{11} = 0, u_{12} = 0, \theta_{11} = 1, \theta_{12} = 0, \omega_{11} = -u_{11}', \omega_{12} = -u_{12}' \text{ at } y = 0 \quad (3.25)$$

$$u_{11} \rightarrow 1, u_{12} \rightarrow 0, \theta_{11} \rightarrow 0, \theta_{12} \rightarrow 0, \omega_{11} \rightarrow 0, \omega_{12} \rightarrow 0 \text{ as } y \rightarrow \infty$$

By solving equations (3.12) - (3.17) under the boundary conditions (3.18), and equations (3.19)-(3.24) under the boundary conditions (3.25), and using equations (3.11) and (3.1), we obtain the velocity, microrotation, temperature and concentration distributions in the boundary layer as

$$\begin{aligned}
u(y) = & a_1 e^{-m_1 y} + a_2 e^{-\Gamma y} + a_3 e^{-Sc y} + a_4 e^{-\eta y} \\
& + Ec \{ a_5 e^{-m_2 y} + a_6 e^{-\Gamma y} + a_7 e^{-2m_2 y} + a_8 e^{-2\Gamma y} + a_9 e^{-2Sc y} + a_{10} e^{-2\eta y} + a_{11} e^{-(m_1 + \Gamma) y} \\
& + a_{12} e^{-(m_1 + Sc) y} + a_{13} e^{-(m_1 + \eta) y} + a_{14} e^{-(\Gamma + Sc) y} + a_{15} e^{-(\Gamma + \eta) y} + a_{16} e^{-(Sc + \eta) y} + a_{17} e^{-\eta y} \} \\
& + \varepsilon e^{m_1} \{ \{ b_2 e^{-m_2 y} + b_3 e^{-m_3 y} + b_4 e^{-m_4 y} + b_5 e^{-m_5 y} \} + Ec \{ b_6 e^{-m_2 y} + b_7 e^{-m_3 y} + b_8 e^{-(m_1 + m_2) y} \\
& + b_9 e^{-(m_1 + m_3) y} + b_{10} e^{-(m_1 + m_4) y} + b_{11} e^{-(m_1 + m_5) y} + b_{12} e^{-(m_1 + \Gamma) y} + b_{13} e^{-(m_1 + \Gamma) y} + b_{14} e^{-(m_1 + \Gamma) y} \\
& + b_{15} e^{-(m_1 + \Gamma) y} + b_{16} e^{-(m_2 + Sc) y} + b_{17} e^{-(m_2 + Sc) y} + b_{18} e^{-(m_2 + Sc) y} + b_{19} e^{-(m_2 + Sc) y} + b_{20} e^{-(m_2 + \eta) y} \\
& + b_{21} e^{-(m_2 + \eta) y} + b_{22} e^{-(m_2 + \eta) y} + b_{23} e^{-(m_2 + \eta) y} + b_{24} e^{-m_1 y} \} \}
\end{aligned}$$

$$\omega(y) = c_1 e^{-\eta y} + Ec \{ c_2 e^{-\eta y} \} + \varepsilon e^{m_1} \{ c_3 e^{-m_2 y} + Ec \{ c_4 e^{-m_1 y} \} \}$$

$$\begin{aligned}
\theta(y) = & e^{-\Gamma y} + Ec \{ c_1 e^{-\Gamma y} + c_2 e^{-2m_2 y} + c_3 e^{-2\Gamma y} + c_4 e^{-2Sc y} + c_5 e^{-2\eta y} + c_6 e^{-(m_1 + \Gamma) y} + c_7 e^{-(m_1 + Sc) y} \\
& + c_8 e^{-(m_1 + \eta) y} + c_9 e^{-(\Gamma + Sc) y} + c_{10} e^{-(\Gamma + \eta) y} + c_{11} e^{-(Sc + \eta) y} \} + \varepsilon e^{m_1} \{ \{ e^{-m_2 y} \} + Ec \{ c_{12} e^{-m_2 y} \\
& + c_{13} e^{-(m_1 + m_2) y} + c_{14} e^{-(m_1 + m_3) y} + c_{15} e^{-(m_1 + m_4) y} + c_{16} e^{-(m_1 + m_5) y} + c_{17} e^{-(m_1 + \Gamma) y} + c_{18} e^{-(m_1 + \Gamma) y} \\
& + c_{19} e^{-(m_1 + \Gamma) y} + c_{20} e^{-(m_2 + \Gamma) y} + c_{21} e^{-(m_2 + Sc) y} + c_{22} e^{-(m_2 + Sc) y} + c_{23} e^{-(m_2 + Sc) y} + c_{24} e^{-(m_2 + Sc) y} \\
& + c_{25} e^{-(m_2 + \eta) y} + c_{26} e^{-(m_2 + \eta) y} + c_{27} e^{-(m_2 + \eta) y} + c_{28} e^{-(m_2 + \eta) y} \} \}
\end{aligned}$$

$$C(y) = e^{-Sc y} + \varepsilon e^{m_1} \{ e^{-m_1 y} \}$$

where

$$m_1 = \frac{1}{2(1+\beta)} \left[1 + \sqrt{1 + 4N(1+\beta)} \right], \quad m_2 = \frac{1}{2(1+\beta)} \left[1 + \sqrt{1 + 4(N+n)(1+\beta)} \right]$$

$$m_3 = \frac{\eta}{2} \left[1 + \sqrt{1 + \frac{4n}{\eta}} \right], \quad m_4 = \frac{\Gamma}{2} \left[1 + \sqrt{1 + \frac{4n}{\Gamma}} \right], \quad m_5 = \frac{Sc}{2} \left[1 + \sqrt{1 + \frac{4n}{Sc}} \right]$$

and the expressions for the remaining constants are given in the appendix.

From the engineering point of view, the most important characteristics of the flow are the skin friction coefficient C_f , couple stress coefficient C_m , Nusselt number Nu and Sherwood number Sh , which are discussed below.

Knowing the velocity field in the boundary layer, we can calculate the skin-friction coefficient C_f at the porous plate, which in the non-dimensional form is given by

$$C_f = \frac{2\tau_w^*}{\rho U_0^* y_0}, \quad \text{where } \tau_w^* = (\mu + \Lambda) \left. \frac{\partial u^*}{\partial y^*} \right|_{y^*=0} + \Lambda w^* \Big|_{y^*=0}$$

3A662

$$\begin{aligned}
 &= 2\{1+(1-n)\beta\} \left[\frac{du}{dy} \right]_{y=0} \\
 &= 2\{1+(1-n)\beta\} \left[\frac{du_{01}}{dy} + Ec \frac{du_{02}}{dy} + \varepsilon e^{\eta y} \left\{ \frac{du_{11}}{dy} + Ec \frac{du_{12}}{dy} \right\} \right]_{y=0} \\
 &= - \left[\begin{aligned}
 &a_1 m_1 + a_2 \Gamma + a_3 Sc + a_4 \eta + Ec \{ a_5 m_1 + a_6 \Gamma + 2a_7 m_1 + 2\Gamma a_8 + 2Sc a_9 + 2\eta a_{10} + a_{11} (m_1 + \Gamma) \} \\
 &+ a_{12} (m_1 + Sc) + a_{13} (m_1 + \eta) + a_{14} (\Gamma + Sc) + a_{15} (\Gamma + \eta) + a_{16} (Sc + \eta) + a_{17} \eta \\
 &+ \varepsilon e^{\eta y} \{ b_2 m_2 + b_3 m_1 + b_4 m_4 + b_5 m_1 \} + Ec \{ b_6 m_2 + b_7 m_4 + b_8 (m_1 + m_2) + b_9 (m_1 + m_3) \\
 &+ b_{10} (m_1 + m_4) + b_{11} (m_1 + m_3) + b_{12} (m_2 + \Gamma) + b_{13} (m_3 + \Gamma) + b_{14} (m_4 + \Gamma) + b_{15} (m_4 + \Gamma) \\
 &+ b_{16} (m_2 + Sc) + b_{17} (m_3 + Sc) + b_{18} (m_4 + Sc) + b_{19} (m_3 + Sc) + b_{20} (m_2 + \eta) + b_{21} (m_3 + \eta) \\
 &+ b_{22} (m_4 + \eta) + b_{23} (m_3 + \eta) + b_{24} m_3 \}
 \end{aligned} \right]
 \end{aligned}$$

Knowing the microrotation in the boundary layer, we can calculate the couple stress coefficient C_m at the porous plate, which in the non-dimensional form is given by

$$\begin{aligned}
 C_m &= \frac{M_w}{\mu \beta U_0}, \text{ where } M_w = \gamma \left. \frac{\partial w'}{\partial y'} \right|_{y'=0} \\
 &= \left(1 + \frac{1}{2} \beta \right) w'(0), \\
 &= - \left(1 + \frac{1}{2} \beta \right) \{ (c_1 + Ec c_2) \eta + (c_3 + Ec c_4) m_1 \}
 \end{aligned}$$

Knowing the temperature field in the boundary layer, we can calculate the heat transfer coefficient at the porous plate, which in terms of the Nusselt number is given by

$$\begin{aligned}
 Nu_x &= x \frac{(\partial T / \partial y')_{y'=0}}{T_w - T_\infty}, \\
 Nu_x Re_x^{-1} &= - \left[\frac{d\theta}{dy} \right]_{y=0} = - \left(\frac{\partial \theta_0}{\partial y} + \varepsilon e^{\eta y} \frac{\partial \theta_1}{\partial y} \right)_{y=0} \\
 &= - \left[\frac{d\theta_{01}}{dy} + Ec \frac{d\theta_{02}}{dy} + \varepsilon e^{\eta y} \left\{ \frac{d\theta_{11}}{dy} + Ec \frac{d\theta_{12}}{dy} \right\} \right]_{y=0}
 \end{aligned}$$

RS
510
R 368



$$\begin{aligned}
&= \Gamma + Ec\{c_1\Gamma + 2m_1c_2 + 2\Gamma c_3 + 2Sc c_4 + 2\eta c_5 + c_6(m_1 + \Gamma + c_7(m_1 + Sc)) + c_8(m_1 + \eta) \\
&+ c_9(\Gamma + Sc) + c_{10}(\Gamma + \eta) + c_{11}(Sc + \eta)\} + \varepsilon e^m\{m_4 + Ec\{c_{12}m_4 + c_{13}(m_1 + m_2) \\
&+ c_{14}(m_1 + m_3) + c_{15}(m_1 + m_4) + c_{16}(m_1 + m_5) + c_{17}(m_2 + \Gamma) + c_{18}(m_3 + \Gamma) + c_{19}(m_4 + \Gamma) \\
&+ c_{20}(m_4 + \Gamma) + c_{21}(m_2 + Sc) + c_{22}(m_3 + Sc) + c_{23}(m_4 + Sc) + c_{24}(m_3 + Sc) + c_{25}(m_2 + \eta) \\
&+ c_{26}(m_3 + \eta) + c_{27}(m_4 + \eta) + c_{28}(m_5 + \eta)\}
\end{aligned}$$

Knowing the concentration field in the boundary layer, we can calculate the mass transfer coefficient at the porous plate, which in terms of the Sherwood number is given by

$$Sh_x = \frac{j_w x}{D^*(C_w^* - C_\infty^*)}, \text{ where } j_w = -D^* \left. \frac{\partial C^*}{\partial y^*} \right|_{y^*=0}$$

$$\begin{aligned}
Sh_x Re_x^{-1} &= - \left[\frac{dC}{dy} \right]_{y=0} = - \left[\frac{dC_0}{dy} + \varepsilon e^m \frac{dC_1}{dy} \right]_{y=0} \\
&= Sc + \varepsilon e^m m_5,
\end{aligned}$$

where $Re_x = \frac{V_0 x}{\nu}$ is the Reynolds number.

4. RESULTS AND DISCUSSION

The formulation of the problem that accounts for the effects of radiation and viscous dissipation on the MHD free convection mass transfer flow of an incompressible, micropolar fluid along an infinite vertical porous moving plate embedded in porous medium is carried out in the preceding sections. This enables us to carry out the numerical computations for the velocity, microrotation, temperature and concentration for various values of the flow and material parameters. In the present study we have chosen $\iota = 1, \varepsilon = 0.01$ and $n = 0.1$, while $\beta, Gr, Gc, M, K, Sc, Pr, R, Up$ and Ec are varied over a range, which are listed in the figure legends.

The effect of viscosity ratio β on the translational velocity and microrotation across the boundary layer are presented in Fig. 1. It is noted that the velocity distribution is lower for a Newtonian fluid ($\beta = 0$) for prescribed values of flow parameters, as compared with that of micropolar fluid. The translational velocity increases near the plate, as the viscosity ratio β increases and then approaches to zero. In addition, the

microrotation increases, with an increase in β near to the plate, but the effect is opposite far away from the plate.

Fig. 2 illustrates the variation of velocity and microrotation distribution across the boundary layer for various values of the plate velocity Up . It is observed that both the translational velocity and microrotation increase, as the plate moving velocity increases.

For different values of the magnetic field parameter M , the translational velocity and microrotation profiles are plotted in Fig 3. It is seen that the velocity distribution across the boundary layer decreases, as M increases. Further, the results show that the values of microrotation increases, as M increases.

For various values of the permeability parameter K , the profiles of the translational velocity and microrotation across the boundary layer are shown in Fig. 4. Clearly as K increases the peak value of velocity across the boundary layer tends to increase rapidly near the porous plate. The results also reveal that the magnitude of microrotation profiles increases, as K increases.

The translational velocity and the microrotation profiles against spanwise coordinate y for different values of Grashof number Gr and modified Grashof number Gc are described in Fig. 5. It is observed that an increase in Gr or Gc leads to a rise in the values of velocity, but a fall in the microrotation. Here the positive values of Gr corresponds to a cooling of the surface by natural convection.

Fig. 6 shows the translational velocity and the microrotation profiles across the boundary layer for different values of the Prandtl number Pr . It is seen that the translational velocity decreases, as Pr increases. Also, it is observed that the magnitude of microrotation increases, as Pr increases.

For different values of the thermal radiation parameter R , the translational velocity, microrotation and temperature profiles are plotted in Fig.7. It is observed that as the radiation parameter R increases, both the velocity and temperature decrease whereas the microrotation increases.

For different values of the Schmidt number Sc , translational velocity and the microrotation profiles are plotted in Fig. 8. It is observed that as Sc increases, the velocity decreases across the boundary layer and the microrotation increases.

The effect of viscous dissipation parameter i.e., Eckert number Ec on the velocity, Microrotation and temperature are shown in Fig.9. It is noticed that as Ec increases, there is an increase in the velocity distribution across the boundary layer and a decrease in both the Microrotation and temperature.

Figs. 10 and 11 illustrate the influence of the Prandtl number Pr and radiation parameter R on the temperature in the boundary layer. From these figures, it is clear that the temperature decreases, as Pr or R increases.

Fig.12 shows the concentration profiles across the boundary layer for various values of Schmidt number Sc . It is seen that as Sc increases, the concentration decreases, because the smaller values of Sc are equivalent to increasing the chemical molecular diffusivity.

Numerical values of the skin-friction coefficient C_f , couple stress coefficient C_m , Nusselt number Nu and Sherwood number Sh are tabulated in Table 1 for different values of thermophysical parameters. Analysis of the tabular data shows that the skin friction coefficient decreases, as β or M or Pr or R increases, whereas it increases, as Gr or Gc or Ec or Sc increases. The couple stress follows same trend. Further, it is observed that the Nusselt number decreases, as β or M or Pr or R increases, whereas it increases, as Gr or Gc or Ec increases. The effect of increasing values of Sc has the tendency to increase the Sherwood number, but the remaining parameters β , M , Gr , Gc , Ec , Pr and R have no effect on the Sherwood number.

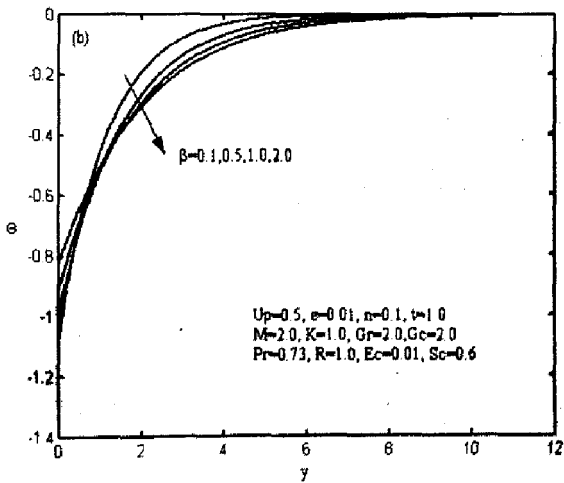
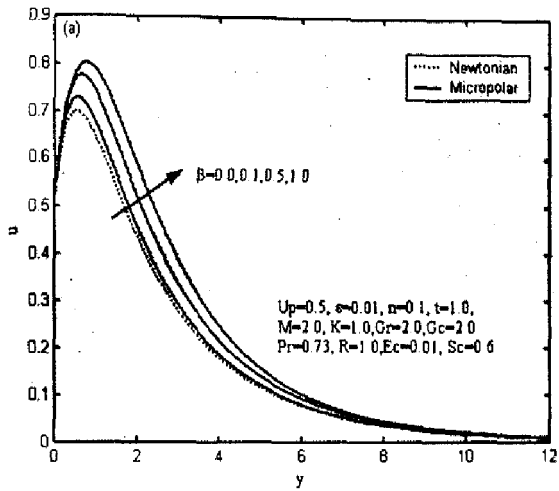


Fig. 1 Velocity and microrotation profiles for various values of β

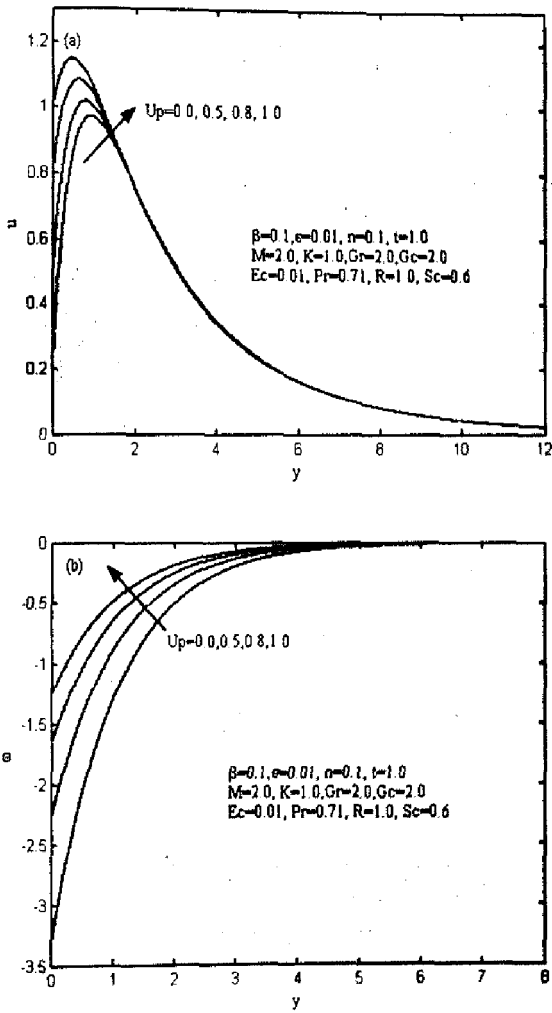


Fig. 2. Velocity and microrotation profiles for various values of U_p

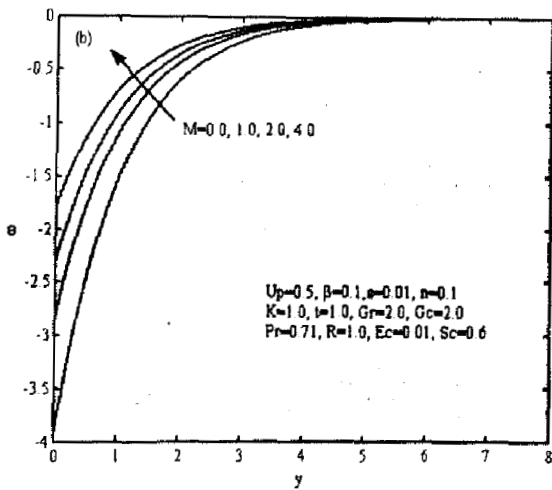
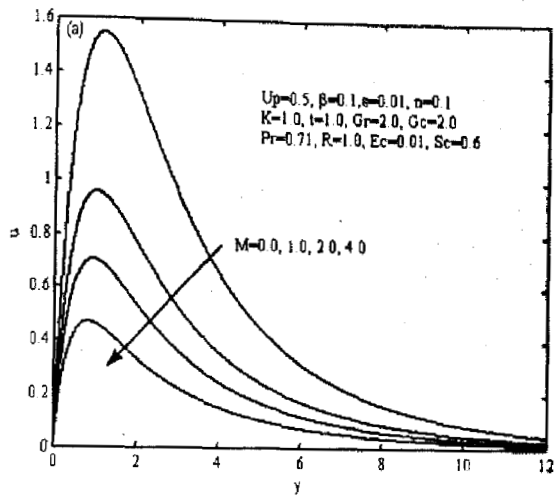


Fig. 3 Velocity and microrotation profiles for various values of M

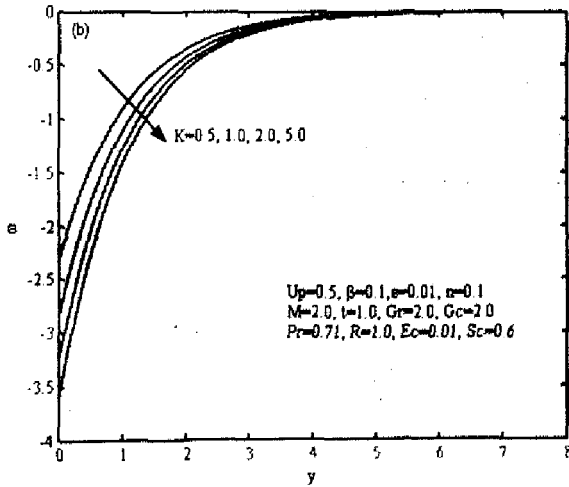
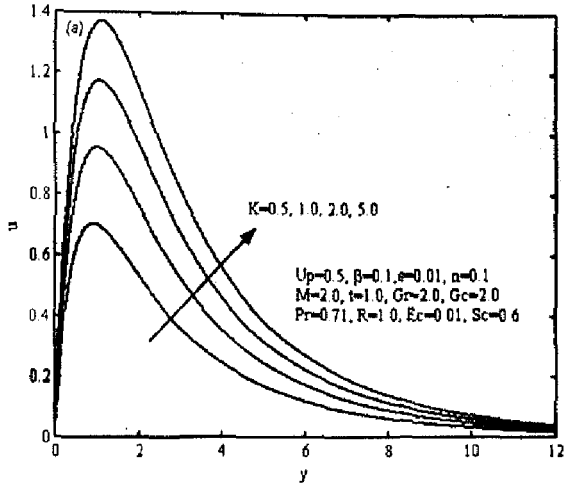


Fig. 4 Velocity and microrotation profiles for various values of K

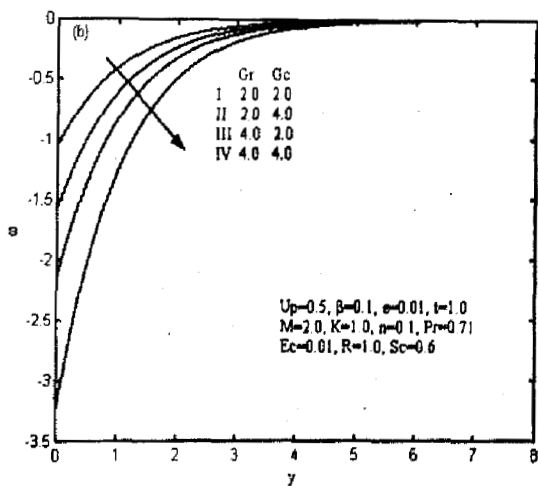
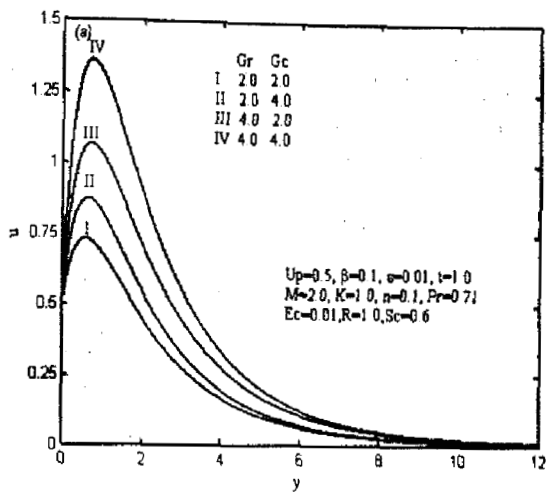


Fig. 5 Velocity and microrotation profiles for various values of Gr & Gc

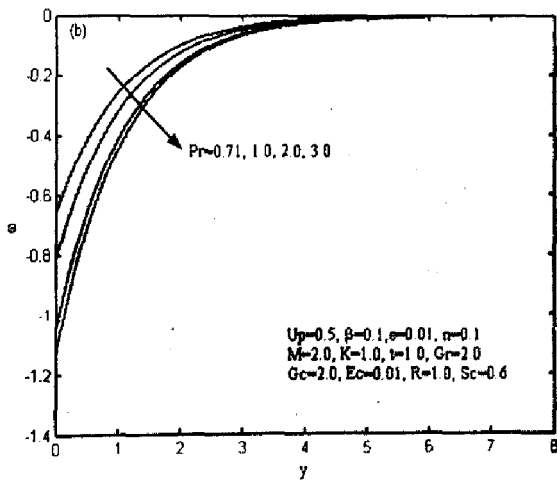
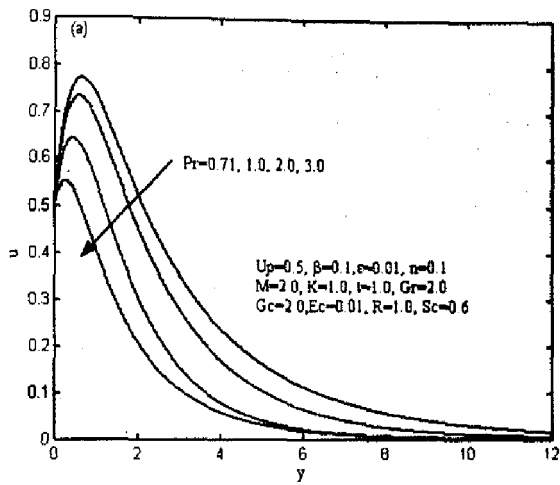


Fig. 6 Velocity and microrotation profiles for various values of Pr

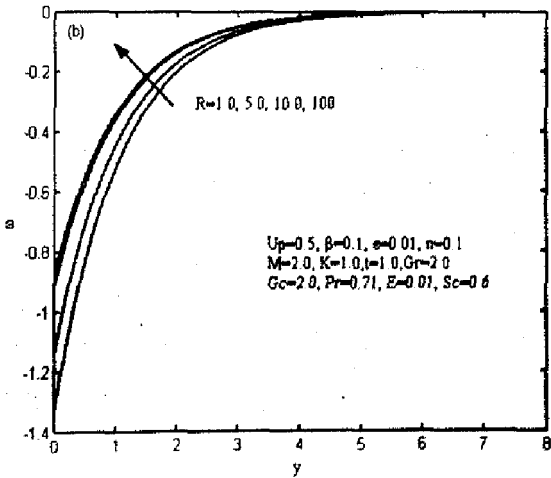
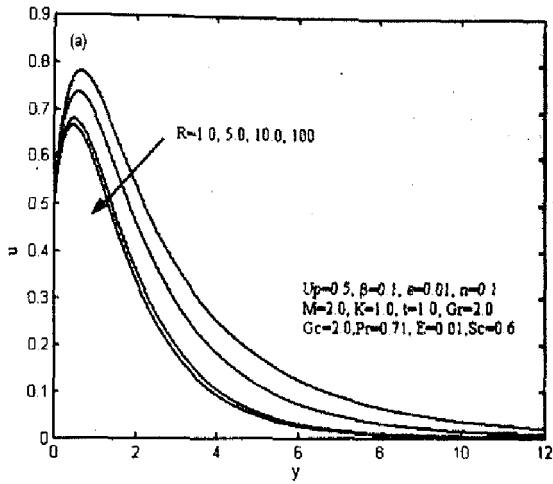


Fig. 7 Velocity and microrotation profiles for various values of R

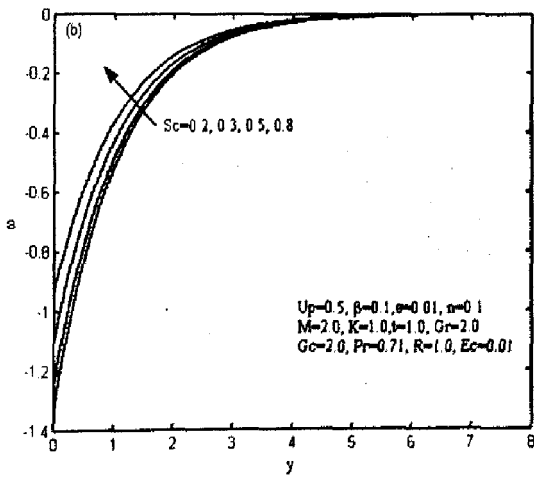
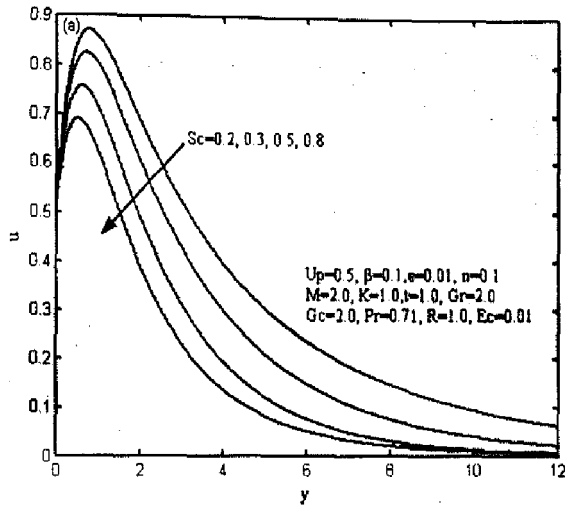


Fig. 8 Velocity and microrotation profiles for various values of Sc

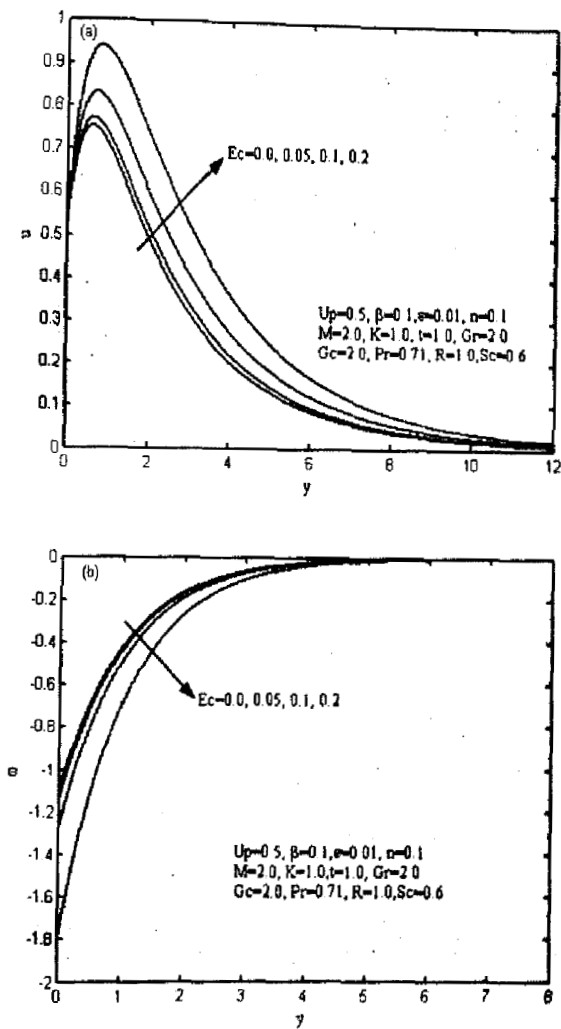


Fig. 9 Velocity and microrotation profiles for various values of Ec

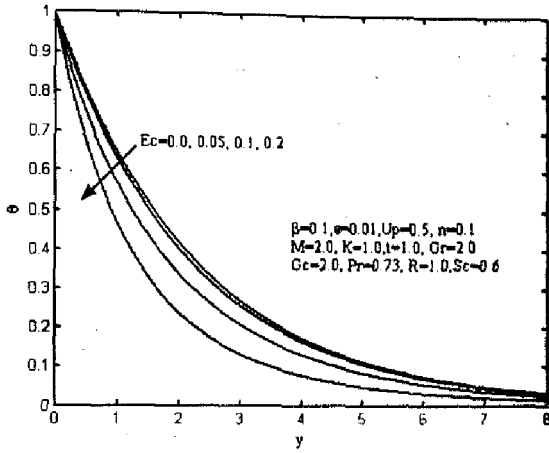


Fig. 9 (c) Temperature profiles for various values of Ec

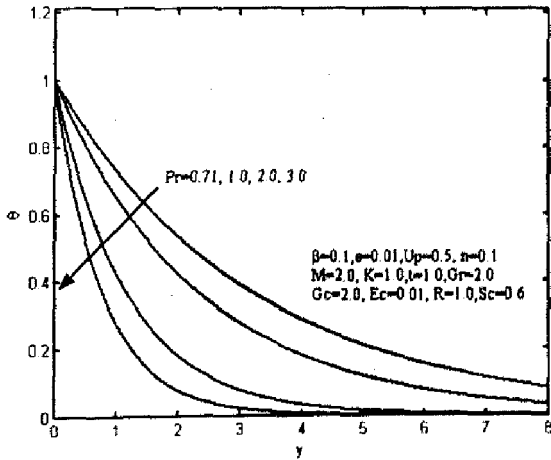


Fig. 10. Temperature profiles for various values of Pr

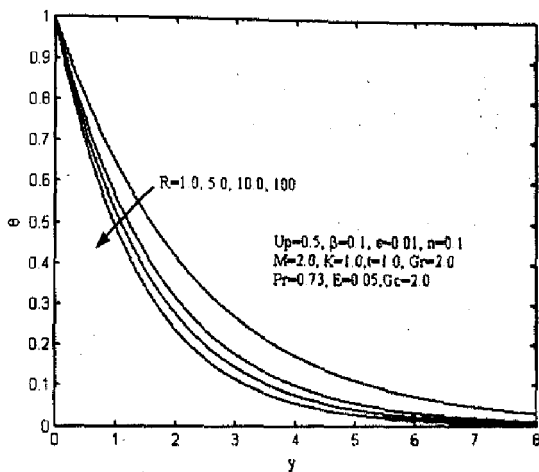


Fig. 11. Temperature profiles for various values of R

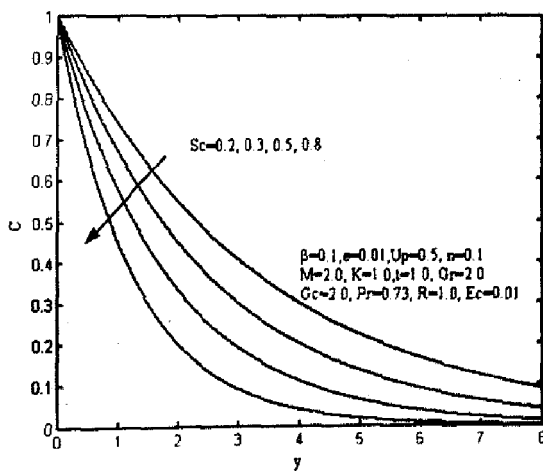


Fig.12 Concentration profiles for various values of Sc

Table 1: Effects of various parameters on C_r , C_m , $Nu Re_1^{-1}$ and $Sh_1 Re_1^{-1}$ for values of β , M , Gr , Gc , Ec , Pr , R , Sc with $t=1$, $n=0.1$, $\epsilon=0.01$ and $U_p=0.5$.

β	M	Gr	Gc	Ec	Pr	R	Sc	C_r	C_m	$Nu Re_1^{-1}$	$Sh_1 Re_1^{-1}$
0.0	2.0	2.0	2.0	0.01	0.71	2.0	0.6	3.3742	3.6832	0.4267	0.6008
0.1								0.6444	0.6446	0.4269	0.6008
0.5								0.5991	0.5990	0.4274	0.6008
0.5	0.0	2.0	2.0	0.01	0.71	2.0	0.6	1.7233	1.7232	0.4265	0.6008
	1.0							1.0339	1.0338	0.4263	0.6008
	2.0							0.5991	0.5990	0.4253	0.6008
0.5	2.0	2.0	2.0	0.01	0.71	2.0	0.6	0.5991	0.5990	0.4253	0.6008
		4.0						1.6116	1.6113	0.4240	0.6008
		6.0						2.6247	2.6244	0.4228	0.6008
0.5	2.0	2.0	2.0	0.01	0.71	2.0	0.6	0.5991	0.5990	0.4253	0.6008
			4.0					1.5199	1.5200	0.4240	0.6008
			6.0					2.4408	2.4410	0.4228	0.6008
0.5	2.0	2.0	2.0	0.01	0.71	2.0	0.6	0.5991	0.5990	0.4253	0.6008
				0.05				0.6068	0.6067	0.3945	0.6008
				1.0				3.8376	3.8434	-12.4087	0.6008
0.5	2.0	2.0	2.0	0.01	0.71	2.0	0.6	0.5991	0.5990	0.4253	0.6008
					1.0			0.5076	0.5075	0.6011	0.6008
					3.0			0.1553	0.1554	1.8037	0.6008
0.5	2.0	2.0	1.0	0.01	0.71	1.0	0.6	0.6740	0.6739	0.3046	0.6008
						2.0		0.5991	0.5990	0.4253	0.6008
						5.0		0.5268	0.5267	0.5617	0.6008
0.5	2.0	2.0	1.0	0.01	0.71	2.0	0.2	0.8389	0.8388	0.4285	0.2003
							0.6	0.5991	0.5990	0.4253	0.6008
							0.8	0.5125	0.5124	0.4265	0.8010

REFERENCES

1. Cheng P. and Minkowycz W. K. (1977), Free convection about a vertical plate embedded in a porous medium with application to heat transfer from a dike, *J. Geophys. Research.*, Vol. 82, pp. 2040–2044.
2. Bejan A. and Khair K. R. (1985), Heat and mass transfer by natural convection in a porous medium, *Int. Commun. Heat Mass Transfer*, Vol. 28, pp. 909–918.
3. Lai F.C. and Kulacki F.A. (1991), Non-Darcy mixed convection along a vertical wall in a saturated porous medium, *Int. J. Heat Mass Transfer*, Vol. 113, pp. 252–255.
4. Bestman A.R. (1990), Natural convection boundary layer with suction and mass transfer in a porous medium, Vol. 14, pp. 389–396.
5. Eringen A.C. (1966), Theory of micropolar fluids, *J. Math. Mech.* Vol 16, pp. 1–18.
6. Eringen A.C. (1972), Theory of thermomicrofluids, *J. Math. Anal. Appl.* Vol 38, pp.480–496.
7. Ariman T., Turk M.A. and Sylvester N.D. (1973), Microcontinuum fluid mechanics, A review, *Int. J. Engg. Sci.* Vol .11, pp.905–930.
8. Ariman T, Turk M.A., and Sylvester N.D. (1974), Applications of microcontinuum fluid mechanics, A review, *Int. J. Eng. Sci.*, Vol .12, pp.273–293.
9. Mansour M.A. and Gorla R.S.R. (1999), Micropolar fluid flow past a continuously moving in the presence of magnetic field, *Appl. Mech. Eng.*, Vol.4, pp. 663–672.
10. El-Hakiem M.A., Mohammadien and A.A., El-Kabeir S.M.M and Gorla R.S.R. (1999), Joule heating effects on MHD free convection flow of a micropolar fluid, *Int. Commun. Heat and Mass Transfer*, Vol. 26(3), pp. 219–227.
11. El-Amin (2001), MHD free convection and mass transfer flow in micropolar fluid with constant suction, *Journal of magnetism and magnetic materials*, Vol. 234, pp. 567–574.
12. Helmy K.A., Idriss H.F. and Kassem S.E. (2002), MHD free convection flow of a micropolar fluid past a vertical porous plate, *Can. J. Phys.*, Vol. 80, pp.1661–1673.
13. Seddeek. M.A. (2003), Flow of a magneto-micropolar fluid past a continuous moving plate, *Physics Letters A*, Vol. 306, pp. 255–257.

14. Kim Y.J. (2004), Heat and mass transfer in MHD micropolar flow over a vertical moving porous plate in a porous medium, Vol. 56, pp. 17–37.
15. Raptis A (1998), Flow of a micropolar fluid past a continuously moving plate by the presence of radiation, *Int. J. Heat Mass Transfer*, Vol. 41, pp. 2865–2866.
16. Kim Y.J. and Fodorov A.G. (2003), Transient radiative convection flow of a micropolar fluid past a moving, semi-infinite vertical porous plate, *Int. J. Heat and Mass Transfer*, Vol. 46, pp.1761-1758.
17. Raptis A. and Perdikis C. (2004), Unsteady flow through high porous medium in the presence of radiation, *Transport in Porous Media*, Vol. 57, pp. 171–179.
18. Rahman M.M. and Sattar M.A.(2007), Transient convective flow of micropolar fluid past a continuously moving vertical porous plate in the presence of radiation, *Int. J. App. Mech. Engi.*, Vol. 12(2), pp. 497–513.
19. Cooney C. I, Omub-Pepple V. B, and Ogulu A (2003), Influence of viscous dissipation and radiation on unsteady MHD free convection flow past an infinite heated vertical plate in a porous medium with time-dependent suction. *Int. J. Heat Mass Transfer*; Vol. 46, pp. 305–311.
20. Ramachandra Prasad V and Bhaskar Reddy N (2007), Radiation and mass transfer effects on an unsteady MHD free convection flow past a heated vertical plate in a porous medium with viscous dissipation. *Theoret. Appl. Mech.*, Vol.34, No.2, pp.135–160.
21. Sankar Reddy T, Gnaneswara Reddy M and Bhaskar Reddy N (2008), Unsteady MHD convective heat and mass transfer flow of micropolar fluid past a semi-infinite vertical moving porous plate in the presence radiation, *Acta Ciencia Indica*, Vol.34(3), pp.1253–1271.
22. Sankar Reddy T, Rama Chandra Prasad V, Roja P and Bhaskar Reddy N (2010), Radiation effects on MHD mixed convection flow of a micropolar fluid past a semi-infinite moving porous plate in a porous medium with heat absorption. *International Journal of Applied Mathematics and Mechanics*, Vol.6 (18), pp.80–101.
23. Gebhart B (1962) "Effect of viscous dissipation in natural convection", *Journal of Fluid Mechanics*, Vol. 14, pp. 225–235.

24. Gebhart B and Mollendorf J (1969), "Viscous dissipation in external natural convection flows", Journal of Fluid Mechanics, vol. 38, pp. 97-107.
25. Cramer K.R. and Pai S.I. (1973), Magneto fluid Dynamics for Engineers and Applied Physicists, Mc Graw Hill, New York.
26. Brewster M. Q. (1992), Thermal radiative Transfer and properties, John Wiley and Sons, New York.

APPENDIX

$$a_1 = U_p - (a_2 + a_3 + a_4), \quad a_2 = \frac{-Gr}{(1+\beta)\Gamma^2 - \Gamma - N}$$

$$a_3 = \frac{-Gc}{(1+\beta)Sc^2 - Sc - N}, \quad a_4 = \frac{2\beta\eta k_1}{(1+\beta)\eta^2 - \eta - N} = \theta_1 k_1$$

$$a_5 = -\sum_{j=5}^{17} a_j, \quad a_6 = \frac{-Gr c_1}{(1+\beta)\Gamma^2 - \Gamma - N}$$

$$a_7 = \frac{-Gr c_2}{4(1+\beta)m_1^2 - 2m_1 - N}, \quad a_8 = \frac{-Gr c_3}{4(1+\beta)\Gamma^2 - 2\Gamma - N}$$

$$a_9 = \frac{-Gr c_4}{4(1+\beta)Sc^2 - 2Sc - N}, \quad a_{10} = \frac{-Gr c_5}{4(1+\beta)\eta^2 - 2\eta - N}$$

$$a_{11} = \frac{-Gr c_6}{(1+\beta)(m_1 + \Gamma)^2 - (m_1 + \Gamma) - N}, \quad a_{12} = \frac{-Gr c_7}{(1+\beta)(m_1 + Sc)^2 - (m_1 + Sc) - N}$$

$$a_{13} = \frac{-Gr c_8}{(1+\beta)(m_1 + \eta)^2 - (m_1 + \eta) - N}, \quad a_{14} = \frac{-Gr c_9}{(1+\beta)(Sc + \Gamma)^2 - (Sc + \Gamma) - N}$$

$$a_{15} = \frac{-Gr c_{10}}{(1+\beta)(\Gamma + \eta)^2 - (\Gamma + \eta) - N}, \quad a_{16} = \frac{-Gr c_{11}}{(1+\beta)(Sc + \eta)^2 - (Sc + \eta) - N}$$

$$a_{17} = \frac{2\beta\eta k_2}{(1+\beta)\eta^2 - 2\eta - N}, \quad b_2 = -(b_3 + b_4 + b_5), \quad b_3 = \frac{2\beta m_3 k_3}{(1+\beta)m_3^2 - m_3 - N}$$

$$b_4 = \frac{-Gr}{(1+\beta)m_4^2 - m_4 - N}, \quad b_5 = \frac{-Gr}{(1+\beta)m_5^2 - m_5 - N}$$

$$b_6 = - \left(\sum_{i=6}^{22} b_i \right)^5, \quad b_7 = \frac{-Gr.C_{12}}{(1+\beta)m_4^2 - \Gamma m_4 - nPr}$$

$$b_8 = \frac{-Gr.C_{13}}{(1+\beta)(m_1+m_2)^2 - \Gamma(m_1+m_2) - n\Gamma}$$

$$b_9 = \frac{-Gr.C_{14}}{(1+\beta)(m_1+m_3)^2 - \Gamma(m_1+m_3) - n\Gamma}$$

$$b_{10} = \frac{-Gr.C_{15}}{(1+\beta)(m_1+m_4)^2 - \Gamma(m_1+m_4) - n\Gamma}$$

$$b_{11} = \frac{-Gr.C_{16}}{(1+\beta)(m_1+m_5)^2 - \Gamma(m_1+m_5) - n\Gamma}$$

$$b_{12} = \frac{-Gr.C_{17}}{(1+\beta)(m_2+\Gamma)^2 - \Gamma(m_2+\Gamma) - n\Gamma}$$

$$b_{13} = \frac{-Gr.C_{18}}{(1+\beta)(m_3+\Gamma)^2 - \Gamma(m_3+\Gamma) - n\Gamma}$$

$$b_{14} = \frac{-Gr.C_{19}}{(1+\beta)(m_4+\Gamma)^2 - \Gamma(m_4+\Gamma) - n\Gamma}$$

$$b_{15} = \frac{-Gr.C_{20}}{(1+\beta)(m_5+\Gamma)^2 - \Gamma(m_5+\Gamma) - n\Gamma}$$

$$b_{16} = \frac{-Gr.C_{21}}{(1+\beta)(m_2+Sc)^2 - \Gamma(m_2+Sc) - n\Gamma}$$

$$b_{17} = \frac{-Gr.C_{22}}{(1+\beta)(m_3+Sc)^2 - \Gamma(m_3+Sc) - n\Gamma}$$

$$b_{18} = \frac{-Gr.C_{23}}{(1+\beta)(m_4+Sc)^2 - \Gamma(m_4+Sc) - n\Gamma}$$

$$b_{19} = \frac{-Gr.C_{24}}{(1+\beta)(m_5+Sc)^2 - \Gamma(m_5+Sc) - n\Gamma}$$

$$b_{20} = \frac{-Gr.C_{25}}{(1+\beta)(m_2+\eta)^2 - \Gamma(m_2+\eta) - n\Gamma}$$

$$b_{21} = \frac{-Gr.C_{26}}{(1+\beta)(m_3+\eta)^2 - \Gamma(m_3+\eta) - n\Gamma}$$

$$b_{22} = \frac{-Gr.C_{27}}{(1+\beta)(m_4+\eta)^2 - \Gamma(m_4+\eta)\Gamma - n\Gamma}$$

$$b_{23} = \frac{-Gr.C_{28}}{(1+\beta)(m_5+\eta)^2 - \Gamma(m_5+\eta) - n\Gamma}$$

$$b_{24} = \frac{2\beta m_3}{(1+\beta)m_3^2 - \Gamma m_3 - n\Gamma} \quad c_1 = -\left(\sum_{i=2}^{11} c_i\right) \quad c_2 = \frac{-\Gamma E a_1^2 m_1^2}{(2m_1)^2 - 2\Gamma m_1}$$

$$c_3 = \frac{-\Gamma E a_2^2 \Gamma Pr}{(2\Gamma)^2 - 2Pr^2} \quad c_4 = \frac{-\Gamma E a_3^2 Sc^2}{(2Sc)^2 - 2\Gamma.Sc} \quad c_5 = \frac{-\Gamma E a_4^2 \eta^2}{(2\eta)^2 - 2\Gamma.\eta}$$

$$c_6 = \frac{-2a_1 m_1 \Gamma a_2 \Gamma E}{(m_1 + \Gamma)^2 - \Gamma(m_1 + \Gamma)} = \frac{-2a_1 a_2 m_1 \Gamma^2 E}{(m_1 + \Gamma)^2 - \Gamma(m_1 + \Gamma Pr)}$$

$$c_7 = \frac{-2a_1 m_1 a_3 Sc \Gamma E}{(m_1 + Sc)^2 - \Gamma(m_1 + Sc)}$$

$$c_8 = \frac{-2a_1 m_1 a_4 \eta Pr E}{(m_1 + \eta)^2 - Pr(m_1 + \eta)} \quad c_9 = \frac{-2\Gamma a_2 a_3 Sc \Gamma E}{(\Gamma + Sc)^2 - \Gamma(\Gamma + Sc)} \quad c_{10} = \frac{-2\Gamma a_2 a_4 \eta \Gamma E}{(\Gamma + \eta)^2 - \Gamma(\Gamma + \eta)}$$

$$c_{11} = \frac{-2a_3 Sc a_4 \eta \Gamma E}{(Sc + \eta)^2 - \Gamma(Sc + \eta)} \quad c_{12} = -\sum_{i=11}^{28} C_i \quad c_{13} = \frac{-2\Gamma E a_1 m_1 b_2 m_2}{(m_1 + m_2)^2 - \Gamma(m_1 + m_2) - n}$$

$$c_{14} = \frac{-2\Gamma E a_1 m_1 b_3 m_3}{(m_1 + m_3)^2 - \Gamma(m_1 + m_3) - n\Gamma} \quad c_{15} = \frac{-2\Gamma E a_1 m_1 b_4 m_4}{(m_1 + m_4)^2 - \Gamma(m_1 + m_4) - n\Gamma}$$

$$c_{16} = \frac{-2\Gamma E a_1 m_1 b_5 m_5}{(m_1 + m_5)^2 - \Gamma(m_1 + m_5) - n\Gamma} \quad c_{17} = \frac{-2\Gamma E a_2 \Gamma b_2 m_2}{(\Gamma + m_2)^2 - \Gamma(\Gamma + m_2) - n\Gamma}$$

$$c_{18} = \frac{-2\Gamma E a_2 \Gamma b_3 m_3}{(\Gamma + m_3)^2 - \Gamma(\Gamma + m_3) - n\Gamma} \quad c_{19} = \frac{-2\Gamma E a_2 \Gamma b_4 m_4}{(\Gamma + m_4)^2 - \Gamma(\Gamma + m_4) - n\Gamma}$$

$$c_{20} = \frac{-2 \Gamma E a_2 \Gamma b_5 m_5}{(\Gamma + m_5)^2 - \Gamma (\Gamma + m_5) - n \Gamma} \quad c_{21} = \frac{-2 \Gamma E a_1 S c b_2 m_2}{(S c + m_2)^2 - \Gamma (S c + m_2) - n \Gamma}$$

$$c_{22} = \frac{-2 \Gamma E a_3 S c b_3 m_3}{(S c + m_3)^2 - \Gamma (S c + m_3) - n \Gamma} \quad c_{23} = \frac{-2 \Gamma E a_1 S c b_4 m_4}{(S c + m_4)^2 - \Gamma (S c + m_4) - n \Gamma}$$

$$c_{24} = \frac{-2 \Gamma E a_3 S c b_5 m_5}{(S c + m_5)^2 - \Gamma (S c + m_5) - n \Gamma} \quad c_{25} = \frac{-2 \Gamma E a_4 \eta b_2 m_2}{(\eta + m_2)^2 - \Gamma (\eta + m_2) - n \Gamma}$$

$$c_{26} = \frac{-2 \Gamma E a_4 \eta b_3 m_3}{(\eta + m_3)^2 - \Gamma (\eta + m_3) - n \Gamma} \quad c_{27} = \frac{-2 \Gamma E a_4 \eta b_4 m_4}{(\eta + m_4)^2 - \Gamma (\eta + m_4) - n \Gamma}$$

$$c_{28} = \frac{-2 \Gamma E a_4 \eta b_5 m_5}{(\eta + m_5)^2 - \Gamma (\eta + m_5) - n \Gamma}$$